

Adaptive Sampling for Rapidly Matching Histograms

Stephen Macke[†], Yiming Zhang[‡], Silu Huang[†], Aditya Parameswaran[†]

University of Illinois-Urbana Champaign

[†]{smacke,shuang86,adityagg}@illinois.edu | [‡]ym_zhang@sjtu.edu.cn

ABSTRACT

In exploratory data analysis, analysts often have a need to identify histograms that possess a specific distribution, among a large class of candidate histograms, e.g., find histograms of countries whose income distribution is most similar to that of Greece. This distribution could be a new one that the user is curious about, or a known distribution from an existing histogram visualization. At present, this process of identification is brute-force, requiring the manual generation and evaluation of a large number of histograms. We present FastMatch: an end-to-end approach for interactively retrieving the histogram visualizations that are most similar to a user-specified target, from a large collection of histograms. The primary technical contribution underlying FastMatch is a sublinear algorithm, HistSim, a theoretically sound sampling-based approach to identify the top- k closest histograms under ℓ_1 distance. While HistSim can be used independently, within FastMatch we couple HistSim with a novel system architecture that is aware of practical considerations, employing block-based sampling policies and asynchronous statistics and computation, building on lightweight sampling engines developed in recent work [36]. In our experiments on several real-world datasets, FastMatch obtains near-perfect accuracy with up to $100\times$ speedups over less sophisticated approaches.

1. INTRODUCTION

In exploratory data analysis, analysts often generate and peruse a large number of visualizations to identify those that *match desired criteria*. This process of iterative “generate and test” occupies a large part of visual data analysis [11, 26, 48], and is often cumbersome and time consuming, especially on very large datasets that are increasingly the norm. This process ends up impeding interaction, preventing exploration, and delaying the extraction of insights.

Example 1: Census Data Exploration. Alice is exploring a census dataset consisting of hundreds of millions of tuples, with attributes such as gender, occupation, nationality, ethnicity, religion, adjusted income, net assets, marital status, number of dependents, and so on. In particular, she is interested in understanding how applying various filters impacts the relative distribution of tuples with different attribute values. She might ask questions like *Q1*: Which countries have similar distributions of wealth to that of Greece? *Q2*: In the United States, which professions have an ethnicity distribution similar to the profession of doctor? *Q3*: Which (country, religion) pairs tend to have a similar distribution of number of children to Christian families in France?

Example 2: Taxi Data Exploration. Bob is exploring the distribution of taxi trip times originating from various locations around Manhattan. Specifically, he plots a histogram showing the distribution of taxi pickup times for trips originating from various

locations. As he varies the location, he examines how the histogram changes, and he notices that choosing the location of a popular nightclub skews the distribution of pickup times heavily in the range of 3am to 5am. He wonders *Q4*: Where are the other locations around Manhattan that have similar distributions of pickup times? *Q5*: Will they all have nightclubs, or are there different reasons for the late-night pickups?

Example 3: Sales Data Exploration. Carol has the complete history of all sales at a large online shopping website. Since users must enter birthdays in order to create accounts, she is able to plot the age distribution of purchasers for any given product. To enhance the website’s recommendation engine, she is considering recommending products with similar purchaser age distributions. To test the merit of this idea, she first wishes to perform a series of queries of the form *Q6*: Which products were purchased by users with ages most closely following the distribution for a certain product—a particular brand of shoes, or a particular book, for example? Carol wishes to perform this query for a few test products before integrating this feature into the recommendation pipeline.

These cases represent scenarios that often arise in exploratory data analysis—finding matches to a specific distribution. The focus of this paper is to *develop techniques for rapidly exploring a large class of histograms to find those that match a user-specified target*.

Referring to *Q1* in the first example, a typical workflow used by Alice may be the following: first, pick a country. Generate the corresponding histogram. This could be done either using a language like R, Python, or Javascript with the visualization generated in ggplot [57] or D3 [12], or using interactions in a visualization platform like Tableau [54]. Does the visualization look similar to that of Greece? If not, pick another, generate it, and repeat. Else, record it, pick another, generate it, and repeat. If only a select few countries have similar distributions, she may spend a huge amount of time sifting through her data, or may simply give up early.

The Need for Approximation. Even if Alice generates all of the candidate histograms (e.g., one for each country) in a single pass, programmatically selecting the closest match to her target (e.g., the Greece histogram), this could take unacceptably long. If the dataset is tens of gigabytes and every tuple in her census dataset contributes to some histogram, then any exact method must necessarily process tens of gigabytes—on a typical workstation, this can take tens of seconds even for in-memory data. By comparison, recent work [40] suggests that latencies greater than 500ms cause significant frustration for end-users and lead them to test fewer hypotheses and potentially identify fewer insights. Thus, in this work, we explore approximate techniques that can return matching histogram visualizations with accuracy guarantees, but much faster.

One tempting approach is to employ approximation using pre-computed samples [6, 5, 4, 9, 24, 22], or pre-computed sketches or

other summaries [14, 47, 61]. Unfortunately, in an interactive exploration setting, pre-computed samples or summaries are not helpful, since the workload is unpredictable and changes rapidly, with more than half of the queries issued one week completely absent in the following week, and more than 90% of the queries issued one week completely absent a month later [45]. In our case, based on the results for one matching query, Alice may be prompted to explore different (and arbitrary) slices of the same data, which can be exponential in the number of attributes in the dataset. Instead, we opt for online sampling, which doesn’t suffer from the same limitations and has been employed for generating approximate visualizations incrementally [50], and while preserving ordering and perceptual guarantees [35, 7]. To the best of our knowledge, however, online approximate query processing techniques have not been applied to the problem of evaluating a large number of visualizations for matches in parallel.

Key Research Challenges. In developing an online-approximation-based approach for rapid histogram matching we immediately encounter a number of theoretical and practical challenges.

1. *Quantifying Importance.* To benefit from approximation, we need to be able to quantify which samples are “important” to facilitate progress towards termination. It is not clear how to assess this importance: at one extreme, it may be preferable to sample more from candidate histograms that are more “uncertain”, but these histograms may already be known to be rather far away from the target. Another approach is to sample more from candidate histograms at the “boundary” of top- k , but if these histograms are more “certain”, refining them further may be useless. Another challenge is when we quantify the importance of samples: one approach would be to reassess importance every time new data become available, but this approach could be computationally costly; or we delay assessment of importance to after every m samples, but this may lead to a state estimate.

2. *Deciding to Terminate.* Our algorithm needs to ascribe a confidence in the correctness of partial results in order to determine when it may safely terminate. This “confidence quantification” requires computation, and if it is slow and/or mismanaged (e.g., if it blocks I/O operations) this computation can actually *increase* the time required for termination over exact methods.

3. *Challenges with Storage Media.* When performing sampling from traditional storage media, the cost to fetch samples is locality-dependent; truly random sampling is extremely expensive due to random I/O, while sampling at the level of blocks is much more efficient, but is less random.

4. *Communication between Components.* It is crucial for our overall system to not be bottlenecked on any component: in quantifying importance (via the sampling manager), deciding whether to terminate (via the statistics manager), and retrieving samples (via the I/O manager). As such, these components must proceed asynchronously, while also minimizing communication across them. Without this, the time taken for execution can often be greater than the time taken by exact methods.

Our Contributions. In this paper, we have developed an end-to-end architecture for histogram matching, dubbed FastMatch, addressing the challenges identified above:

0. *Distance Computation for a Single Histogram.* We prove an information-theoretically optimal upper bound on the number of samples needed for an empirically-learned discrete distribution to be ε -close (under ℓ_1 distance) to the true discrete distribution from which it was sampled. Our FastMatch system uses this guarantee to obtain bounds on the distance of a distribution from an analyst-

provided target. In particular, this bound is tighter than, and therefore more useful than those derived in prior work in the theory literature. (We discuss this further in Section 3.4.)

1. *Importance Quantification Policies.* We develop a sampling engine that employs a simple and theoretically well-motivated criterion for deciding whether processing particular portions of data will allow for faster termination. Since the criterion is simple, it is *easy to update* as we process new data, “understanding” when it has seen enough data for some histogram, or when it needs to take more data to distinguish histograms that are close to each other.

2. *Termination Algorithm.* We develop a statistics engine that repeatedly performs a lightweight “safe termination” test, based on the idea of relaxing fixed-width confidence intervals into variable-width deviation bounds. This relaxation allows these deviation bounds to borrow statistical strength from each other, minimizing the time necessary for safe termination. Since this test is extremely efficient (asymptotically dominated by a distance computation for each histogram), the statistics engine is able to run this frequently enough to ensure timely termination.

3. *Locality-aware Sampling.* To better exploit locality of storage media, FastMatch samples at the level of blocks, proceeding sequentially. To estimate the benefit of blocks, we develop a just-in-time lookahead technique for deciding which blocks to read, in a cache-conscious manner, evaluating the blocks in the same order as their layout in storage. Our technique minimizes the time required for the query output to satisfy our probabilistic guarantees.

4. *Decoupling Components.* Our system decouples the overhead of computation required for allowing safe, early termination (with results satisfying probabilistic guarantees) from the actual I/O involved in sampling. As such, the computation cannot block I/O. Furthermore, we minimize communication overhead introduced by this decoupling using some smart but simple optimizations that exploit the fact that we are dealing with histograms.

Overall, we implement FastMatch within the context of a bitmap-based sampling engine, which allows us to quickly determine whether a given disk block contains samples matching ad-hoc predicates. Bitmap-based sampling engines were found to effectively support approximate generation of visualizations in recent work [7, 35, 50].

We find that our approximation-based techniques working in tandem with our novel systems components *lead to speedups ranging from $7\times$ to over $100\times$* over exact methods, and moreover, unlike less-sophisticated variants of FastMatch, whose performance can be highly data-dependent, FastMatch consistently brings latency to near-interactive levels.

Related Work. To the best of our knowledge, there has been no work on sampling to identify visualizations (in our case, histograms) that match user specifications. Sampling-based techniques have been applied to generate visualizations that preserve visual properties [7, 35], and for incremental generation of time-series and heat-maps [50]—all focusing on the generation of a single visualization. Similarly, Pangloss [44] employs approximation via the Sample+Seek approach [22] to generate a single visualization early, while minimizing error. M4 uses rasterization without sampling to reduce the dimensionality of a time-series visualization and generate it faster [33]. SeeDB [55] recommends visualizations to help distinguish between two subsets of data while employing approximation. However, their objectives are different, and their approach does not provide any guarantees.

Recent work has developed *zenvisage* [52], a visual exploration interface plus language, ZQL, to allow for more expressive querying of visualizations, including operations that identify visualiza-

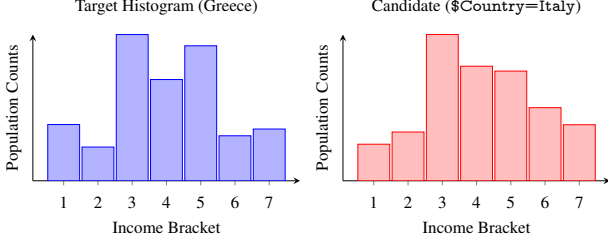


Figure 1: Example visual target and candidate histogram tions (from a large pool of candidates) that are similar to a target. However, to identify matches, *zenvisage* does not consider sampling, and requires at least one complete pass through the dataset. *FastMatch* was developed as a back-end with such interfaces in mind to support rapid discovery of relevant visualizations.

Outline. This paper is organized as follows: Section 2 articulates the formal problem of identifying top- k closest histograms to a target. Section 3 introduces our approximation-based algorithm for solving this problem, while Section 4 describes the system architecture that implements this algorithm. In Section 5 we perform an empirical evaluation on several real-world datasets. After surveying additional related work in Section 6, we describe several generalizations and extensions of our techniques in Appendix A.

2. PROBLEM FORMULATION

In this section, we formalize the problem of identifying histograms whose distributions match a reference. We first discuss how these histograms are generated, and then we define other key concepts and notation.

2.1 Generation of Histograms

We start with a concrete example of the typical database query an analyst might use to generate a histogram. Returning to our example from Section 1, suppose an analyst is interested in studying how population proportions vary across income brackets for various countries around the world. Suppose she wishes to find countries with populations distributed across different income brackets most similarly to a specific country, such as Greece. Consider the following SQL query, where $\$COUNTRY$ is a variable:

```
SELECT income_bracket, COUNT(*) FROM census
WHERE country = $COUNTRY
GROUP BY income_bracket
```

This query returns a list of 7 (income bracket, count) pairs to the analyst for a specific country. The analyst may then choose to visualize the results by plotting the counts versus different income brackets in a histogram, i.e., a plot similar to the right side of Figure 1 (for Italy). Currently, the analyst may examine hundreds of similar histograms, one for each country, comparing it to the one for Greece, to manually identify ones that are similar.

In contrast, the goal of *FastMatch* is to perform this search automatically, efficiently, and online. Conceptually, *FastMatch* will iterate over all possible values of country, generate the corresponding histograms, and evaluate the similarity of its distribution (based on some notion of similarity described subsequently) to the corresponding visualization for Greece. In actuality, *FastMatch* will perform this search all at once, and in an online fashion, quickly pruning countries that are either clearly close or far from the target.

Candidate Visualizations. Formally, we consider visualizations as being generated as a result of **histogram-generating queries**:

DEFINITION 1. A histogram-generating query is a SQL query of the following type:

```
SELECT X, COUNT(*) FROM T
WHERE Z = z_i GROUP BY X
```

The table T and attributes X and Z form the query’s template.

For each concrete value z_i of attribute Z specified in the query, the results of the query—i.e., the grouped counts—can be represented in the form of a vector (r_1, r_2, \dots, r_n) , where $n = |V_X|$, the cardinality of the value set of attribute X . This n -tuple can then be used to plot a histogram visualization—in this paper, when we refer to a histogram or a visualization, we will be typically referring to such an n -tuple. For a given *grouping attribute* X and a *candidate attribute* Z , we refer to the set of all visualizations generated by letting Z vary over its value set as the set of **candidate visualizations**. We refer to each distinct value in the grouping attribute X ’s value set as a *group*. In our example, X corresponds to *income_bracket* and Z corresponds to *country*.

For ease of exposition, we focus on candidate visualizations generated from queries according to Definition 1, having single attributes for X and Z . We note that our methods are more general and extend naturally to handle (i) *predicates*: additional predicates on other attributes, (ii) *multiple and complex Xs*: additional grouping (i.e., X) attributes or groups derived from binning real-values (as opposed to categorical X), and (iii) *multiple and complex Zs*: additional candidate-generating (i.e., Z) attributes. Note that the flexibility in specifying histogram-generating queries—exponential in the number of attributes—makes it impossible for us to precompute the results of all such queries.

Visualization Terminology. We note that our methods are agnostic to the particular method used to present visualizations. That is, analysts may choose to present the results generated from queries of the form in Definition 1 via line plots, heat maps, choropleths, and other visualization types, as any of these may be specified by an ordered tuple of real values and are thus permitted under our notion of a “candidate visualization”. We focus on bar charts of frequency counts and histograms for plotting query results in this paper—these naturally capture aggregations over the categorical or binned quantitative grouping attribute X respectively. Although a bar graph plot of frequency counts over a categorical grouping attribute is not technically a histogram, which implies that the grouping attribute is continuous, we loosely use the term “histogram” to refer to both cases in a unified way.

Visual Target Specification. Given our specification of candidate visualizations, a **visual target** is an n -tuple, denoted by \vec{Q} with entries Q_1, Q_2, \dots, Q_n , that we need to match the candidates with. Returning to our flight delays example, \vec{Q} would refer to the visualization corresponding to Greece, with Q_1 being the count of individuals in the first income bracket, Q_2 the count of individuals in the second income bracket, and so on.

Samples. To estimate these candidate visualizations, we need to take *samples*. In particular, for a given candidate i for some attribute Z , a sample corresponds to a single tuple t with attribute value $Z = z_i$. The attribute value $X = x_j$ of t increments the j th entry of the estimate \vec{r}_i for the candidate histogram.

Candidate Similarity. Given a set of candidate visualizations with estimated vector representations $\{\vec{r}_i\}$ such that the i th candidate is generated by selecting on $Z = z_i$, our problem hinges on finding the candidate whose distribution is most “similar” to the visual target \vec{Q} specified by the analyst. For quantifying visual similarity, we do not care about the absolute counts $r_1, r_2, \dots, r_{|V_X|}$, and instead prefer to determine whether \vec{r}_i and \vec{Q} are close in a *distributional* sense, as described below.

Symbol(s)	Description
X, Z, V_X, V_Z, T	x-axis attribute, candidate attribute, respective value sets, and relation over these attributes, used in histogram-generating queries (see Definition 1)
k, δ, ε	User-supplied parameters (number of matching histograms to retrieve, error probability upper bound, approximation upper bound)
$\vec{Q}, \vec{r}_i, \vec{r}_i^*, (\vec{Q}, \vec{r}_i, \vec{r}_i^*)$	Visual target, candidate i 's estimated (unstarred) and true (starred) histogram counts (normalized variants)
$d(\cdot, \cdot)$	Distance function, used to quantify visual distance (see Definition 2)
$n_i, \varepsilon_i, \delta_i, \tau_i (\tau_i^*)$	Quantities specific to candidate i during HistSim run: number of samples taken, deviation bound (see Definition 4), confidence upper bound on ε_i -deviation, and distance estimate from \vec{Q} (true distance from \vec{Q}), respectively
M	Set of matching histograms during a run of HistSim (see Definition 3)

Table 1: Summary of notation.

To set up distributional distance metrics, we need to first define the normalized variants of \vec{r}_i and \vec{Q} , denoted with hats:

$$\hat{\vec{r}}_i = \frac{\vec{r}_i}{\mathbf{1}^T \vec{r}_i} \quad \hat{\vec{Q}} = \frac{\vec{Q}}{\mathbf{1}^T \vec{Q}}$$

With this notational convenience, we make our notion of similarity explicit by defining candidate distance as follows:

DEFINITION 2. For candidate \vec{r}_i and visual predicate \vec{Q} , the distance $d(\vec{r}_i, \vec{Q})$ between \vec{r}_i and \vec{Q} is defined as follows:

$$d(\vec{r}_i, \vec{Q}) = \|\hat{\vec{r}}_i - \hat{\vec{Q}}\|_1 = \left\| \frac{\vec{r}_i}{\mathbf{1}^T \vec{r}_i} - \frac{\vec{Q}}{\mathbf{1}^T \vec{Q}} \right\|_1$$

That is, after normalizing the candidate and target vectors so that their respective components sum to 1 (and therefore correspond to distributions), we take the ℓ_1 distance between the two vectors. When the target \vec{Q} is understood from context, we denote the distance between candidate \vec{r}_i and \vec{Q} by $\tau_i = d(\vec{r}_i, \vec{Q})$.

The Need for Normalization. A natural question that readers may have is why we chose to normalize each vector prior to taking the distance between them. The reason for this normalization is that the goal of FastMatch is to find visualizations that have similar distributions, as opposed to similar actual values. Returning to our example, if we consider the population distribution of Greece across different income brackets, and compare it to that of other countries, without normalization, we will end up returning other countries with similar population counts in each bin—e.g., other countries with similar overall populations—as opposed to those that have similar shape or distribution. A similar metric, using ℓ_2 distance between normalized vectors (as opposed to ℓ_1), has been studied in prior work [55, 22] and even validated in a user study in [55]. However, as observed in [10], the ℓ_2 distance between distributions has the drawback that it could be small even for distributions with disjoint support. The ℓ_1 distance metric over discrete probability distributions has a direct correspondence with the traditional statistical distance metric known as *total variation distance* [25] and does not suffer from this drawback, so we prefer it in this work.

2.2 Guarantees and Problem Statement

Since FastMatch takes samples to estimate the candidate histogram visualizations, and therefore may return incorrect results, we need to enforce probabilistic guarantees on the correctness of the returned results.

First, we introduce some notation: we use \vec{r}_i to denote the *estimate* of the candidate visualization, while \vec{r}_i^* (with normalized version $\hat{\vec{r}}_i^*$) is the *true* candidate visualization that one would obtain using the entire dataset. Our formulation also relies on constants ε and δ , which we assume given (i.e., either built into the system or provided by the analyst).

GUARANTEE 1. (SEPARATION) Any histogram \vec{r}_j^* that is in the true top- k closest (w.r.t. Definition 2) but not part of the output will be less than ε closer to the target than the furthest histogram that is part of the output. That is, if the algorithm outputs histograms $\vec{r}_{i_1}, \vec{r}_{i_2}, \dots, \vec{r}_{i_k}$, then $\max_{1 \leq l \leq k} \{d(\vec{r}_{i_l}^*, \vec{Q})\} - d(\vec{r}_j^*, \vec{Q}) < \varepsilon$.

Algorithm 1: The high-level HistSim algorithm

Input : Candidate column Z , visual target \vec{Q} , parameters k, ε, δ
Output : An estimate M of the top- k closest candidates to \vec{Q}

```

1
2 Initialization.
3  $n_i \leftarrow 0$  for  $1 \leq i \leq |V_Z|$ ;
4  $\delta^{upper} \leftarrow 1$ ;
5
6 while  $\delta^{upper} > \delta$  do
7   Take some samples;
8   Update  $\{n_i\}, \{\vec{r}_i\}, \{\tau_i\}$ , and  $M$  based on the new samples;
9   Choose  $\{\varepsilon_i\}$  such that Guarantee 1 Guarantee 2 both hold;
10   $\delta^{upper} \leftarrow 0$ ;
11  for  $1 \leq i \leq |V_Z|$  do
12    Let  $\delta_i$  be an upper bound on the probability candidate  $i$  does not have
13     $\varepsilon_i$ -deviation after taking  $n_i$  uniform random samples;
14     $\delta^{upper} \leftarrow \delta^{upper} + \delta_i$ ;
15  end
16 return  $M$ , the currently estimated top- $k$  candidates;

```

GUARANTEE 2. (RECONSTRUCTION) Each approximate histogram \vec{r}_i constructed from empirical counts and output as one of the top- k satisfies $d(\vec{r}_i, \vec{r}_i^*) < \varepsilon$.

The first guarantee says that any ordering mistakes are relatively innocuous: for any two histograms \vec{r}_i and \vec{r}_j , if the algorithm outputs \vec{r}_i but not \vec{r}_j , when it should have been the other way around, then $|d(\vec{r}_i^*, \vec{Q}) - d(\vec{r}_j^*, \vec{Q})| < \varepsilon$. Therefore, we will still be returning a visualization that is “pretty” similar to \vec{Q} . The second guarantee says that the histograms output are not too dissimilar from the corresponding true distributions that would result from a complete scan of the data. As a result, they form an adequate and accurate proxy from which insights may be derived and decisions may be made. With these definitions in place, we now formally state our core problem:

PROBLEM 1. (TOP-K-SIMILAR). Given a visual target \vec{Q} , a histogram-generating query template, k, ε , and δ , display k candidate attribute values $\{z_i\} \subseteq V_Z$ (and accompanying visualizations $\{\vec{r}_i\}$) as quickly as possible, such that the output satisfies Guarantee 1 Guarantee 2 with probability greater than $1 - \delta$.

3. THE HISTSIM ALGORITHM

In this section, we discuss how to conceptually solve Problem 1. We outline an extensible algorithm, named HistSim, which allows us to determine confidence levels for whether our separation and reconstruction guarantees hold. We note that many systems-level details have intentionally been omitted and will be addressed in Section 4. Please refer to Table 1 in Section 2 for a description of the notation used.

3.1 Algorithm Outline

HistSim operates by sampling tuples. Each of these tuples contributes to one or more candidate histograms, using which HistSim constructs histograms $\{\vec{r}_i\}$. After taking enough samples corresponding to each candidate, it will eventually be likely that $d(\vec{r}_i, \vec{r}_i^*)$

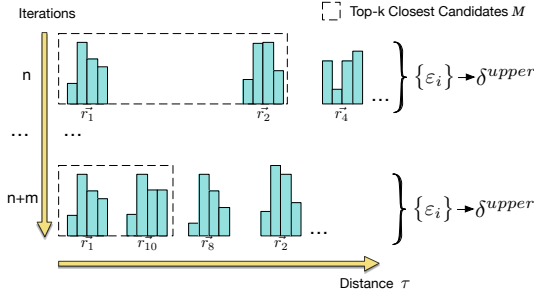


Figure 2: Illustration of HistSim.

is “small”, and that $|d(\vec{r}_i, \vec{Q}) - d(\vec{r}_i^*, \vec{Q})|$ is likewise “small”, for each i . More precisely, the set of candidates will likely be in a state such that Guarantees 1 and 2 are both satisfied simultaneously.

In slightly more detail, this is accomplished at a high level by dividing query processing into “rounds”. Each round consists of an I/O phase, during which tuples are sampled (line 7 in Algorithm 1)—we will describe how subsequently. This is followed by updating, for each candidate, the number of samples n_i , the estimate \vec{r}_i , and the estimated distance τ_i , as well as the current top k candidates, M (line 8). Then, we assign upper bounds ε_i for how far \vec{r}_i is away from the actual \vec{r}_i^* for each candidate such that Guarantees 1 and 2 are met—this is the most involved step of our algorithm and the focus of most of this section (line 9). Subsequently, we compute the upper bound δ^{upper} on the probability that any candidate i violates its assigned deviation ε_i (lines 10–14). As soon as this probability is smaller than δ , we can safely terminate.

Figure 2 illustrates HistSim running on a toy example in which we compute top-2 closest histograms to a target. At round n , it estimates \vec{r}_1 and \vec{r}_2 as the top-2 closest, which it refines by the time it reaches round $n + m$. As the rounds increase and HistSim takes more samples, δ^{upper} decreases.

An artifact of our computation in line 9 is that we can determine which candidates are more “important” to sample from in order to facilitate termination with fewer samples, which can then guide the execution of FastMatch; we return to this in Section 4. Our HistSim algorithm is agnostic to the sampling approach.

Next, in Section 3.2, we prove a lemma that, given appropriate ε_i bounds, allows us to infer the two guarantees; then, in Section 3.3, we describe a method to select those appropriate ε_i ; and in Section 3.4, we prove a theorem that enables us to use the samples per candidate histogram to derive an estimate of ε_i . Finally, in Section 3.5, we conclude with an overall proof of correctness.

3.2 Deviation-Bounds Implies Guarantees

To derive our lemma, we need to first introduce some definitions and notation. We begin with the notion of a *matching* candidate:

DEFINITION 3. (MATCHING CANDIDATES) *During a run of HistSim, a candidate i is called matching if its distance estimate $\tau_i = d(\vec{r}_i, \vec{Q})$ is among the k smallest out of all candidates.*

We denote the set of candidates that are matching during a certain run of HistSim as M ; we likewise denote the true set of matching candidates as M^* . Next, we introduce the notion of ε_i -deviation.

DEFINITION 4. (ε_i -DEVIATION) *During a run of HistSim, a candidate i has a deviation of ε_i if the empirical distribution \vec{r}_i representing its histogram visualization is less than ε_i far from the exact distribution \vec{r}_i^* . That is, $d(\vec{r}_i, \vec{r}_i^*) = \|\vec{r}_i - \vec{r}_i^*\|_1 < \varepsilon_i$*

Note that Definition 4 overloads the symbol ε to be candidate-specific by appending a subscript. In Section 3.4, we provide a way to quantify ε_i given samples.

Now, notice that if HistSim reaches a state where, for each matching candidate $i \in M$, candidate i has ε_i -deviation, and $\varepsilon_i < \varepsilon$ for all $i \in M$, then it is easy to see that the reconstruction guarantee holds for the matching candidates. That is, in such a state, if HistSim output the histograms corresponding to the matching candidates, they would look similar to the true histograms.

Next, in order to reason about the separation guarantee, notice that if candidate i has ε_i -deviation, then the estimate of the distance from the target \vec{Q} , τ_i , must be ε_i -close to the true target distance τ_i^* , via a simple application of the triangle inequality:

LEMMA 1 (DEVIATION-TO-RECONSTRUCTION). *Suppose candidate i has ε_i -deviation. Let $\tau_i = d(\vec{r}_i, \vec{Q})$ be the distance between i ’s empirical counts and the target \vec{Q} . Then $|\tau_i - \tau_i^*| < \varepsilon_i$.*

PROOF. Applying the triangle inequality for differences, we have

$$|\tau_i - \tau_i^*| = \left| \|\vec{r}_i - \vec{Q}\|_1 - \|\vec{r}_i^* - \vec{Q}\|_1 \right| \leq \|\vec{r}_i - \vec{r}_i^*\|_1 < \varepsilon_i$$

where the final inequality comes from the definition of ε_i -deviation. \square

Given this lemma, and the previous observation, we can now show that the notion of ε_i -deviation gives us a mechanism to ensure that *both* the separation and reconstruction guarantees hold. In particular, the following lemma gives two conditions on the deviations $\{\varepsilon_i\}$, that, when satisfied, imply that both guarantees hold.

LEMMA 2 (DEVIATION-TO-GUARANTEES). *Suppose for some set of $\{\varepsilon_i\}$, we know that each candidate i has ε_i -deviation. Guarantees 1 and 2 must hold under the constraints*

$$\max_{i \in M} \{\tau_i + \varepsilon_i\} - \max_{j \notin M} \left\{ \min_{j \notin M} \{\tau_j - \varepsilon_j\}, 0 \right\} < \varepsilon \quad (1)$$

$$\forall i \in M, d(\vec{r}_i, \vec{r}_i^*) < \varepsilon \quad (2)$$

In particular, satisfaction of Equation (1) implies Guarantee 1 holds, and satisfaction of Equation (2) implies Guarantee 2 holds.

Intuitively, constraint 1 allows the ranges that τ_i can lie in for M and for M^* to overlap by at most ε , taking into account that valid overlap cannot be in a nonsensical region of “negative distance”.

PROOF. Notice that Equation (2) implies that Guarantee 2 holds by definition. We now show that satisfaction of Equation (1) implies that Guarantee 1 holds.

If $M = M^*$, the separation guarantee holds trivially and we have nothing to show. Otherwise, suppose $M \neq M^*$, and consider any pair of candidates p and q with $p \in M \setminus M^*$ and $q \in M^* \setminus M$. Since p and q have ε_p - and ε_q -deviation, respectively, we have that

$$\tau_p^* - \tau_q^* \leq \tau_p + \varepsilon_p - \max\{\tau_q - \varepsilon_q, 0\} \quad (1)$$

$$\leq \max_{i \in M} \{\tau_i + \varepsilon_i\} - \max_{j \notin M} \left\{ \min_{j \notin M} \{\tau_j - \varepsilon_j\}, 0 \right\} < \varepsilon \quad (2)$$

The first step follows from application of Lemma 1, which gives $\tau_p^* - \tau_p \leq \varepsilon_p$ and $\tau_q - \tau_q^* \leq \varepsilon_q$, so that $\tau_p^* \leq \tau_p + \varepsilon_p$ and $\tau_q^* \geq \tau_q - \varepsilon_q$, respectively. Furthermore, since τ_q^* is a distance, we must also have $\tau_q^* \geq 0$, yielding $\tau_q^* \geq \max\{\tau_q - \varepsilon_q, 0\}$. The second step follows since $M \setminus M^* \subseteq M$ implies $\tau_p + \varepsilon_p \leq \max_{i \in M} \{\tau_i + \varepsilon_i\}$ and $M^* \setminus M \subseteq \bar{M}$ implies $\tau_q - \varepsilon_q \geq \min_{j \notin M} \{\tau_j - \varepsilon_j\}$. The last step follows from the hypothesis of the lemma. Since p and q were arbitrary mismatched candidates, and their true distances are within ε of each other, the separation guarantee holds. \square

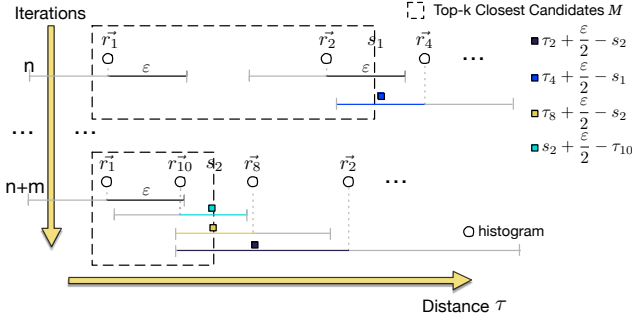


Figure 3: Illustration of how HistSim chooses deviations when trying to determine when the separation and reconstruction guarantees hold w.h.p.

3.3 Selecting the Right Deviations

The most cryptic part of Algorithm 1 is the portion in line 9, which selects the $\{\epsilon_i\}$ such that the constraints of Lemma 2 are satisfied. In particular, it tries to select them in such a way *so as to minimize* δ^{upper} while simultaneously satisfying these constraints. Toward this end, note that it is more likely that $d(\vec{r}_i, \vec{r}_j^*) < \epsilon_i$ when ϵ_i is larger, so it tries to pick the set of $\{\epsilon_i\}$ such that each ϵ_i is as large as possible, under the constraints imposed by Lemma 2.

Ensuring that constraint 2 of the lemma is met is trivial and just involves making sure $\epsilon_i \leq \epsilon$ for $i \in M$. Ensuring that constraint 1 is met is a bit more involved. To do so, we first select a value $s \in [\max_{i \in M} \{\tau_i\}, \min_{j \notin M} \{\tau_j\}]$. Then, for $i \in M$, it ensures that $\tau_i + \epsilon_i \leq s + \frac{\epsilon}{2}$, and for $j \notin M$, it ensures that $\tau_j - \epsilon_j \geq \max\{s - \frac{\epsilon}{2}, 0\}$.

Figure 3 illustrates this choice of the $\{\epsilon_i\}$ on our toy example. As in Figure 2, the boundary of M is represented by the dashed box. The split point s is located at the rightmost boundary of the dashed box — for each candidate j , ϵ_j does not cross s by an amount more than $\frac{\epsilon}{2}$. Furthermore, for candidates in M (inside the box), ϵ_i is further chosen to be smaller than ϵ .

There is still one degree of freedom we have not discussed: namely, how to choose the split point s . Ideally, we could try and choose s such that the $\{\epsilon_i\}$ picked by Algorithm 1 would minimize δ^{upper} . However, in the interest of simplicity and computational ease, we simply choose the midpoint halfway between the furthest candidate in M and the closest candidate not in M . For example, at iteration n in Figure 3, s lies halfway between candidates \vec{r}_2 and \vec{r}_4 .

3.4 Deviation-Bounds Given Samples

The previous section provides us a way to select the ϵ_i deviation for each candidate such that we can achieve the desired guarantees. We now provide a theorem that allows us to infer, given the samples taken for a given candidate, how to relate ϵ_i with the probability δ_i with which the candidate can fail to respect its deviation-bound ϵ_i .

The proof relies on repeated application of the method of bounded differences [43] in order to exploit some special structure in the ℓ_1 distance metric. The bound developed is *information-theoretically optimal*; that is, it takes asymptotically the fewest samples required to guarantee that an empirical distribution estimated from the samples will be no further than ϵ_i from the true distribution. Furthermore, we observe that our bound empirically requires fewer samples to make the same guarantee as the information-theoretical bound noted in [56]. We will return to this point after the proof.

THEOREM 1. *Suppose we have taken n_i samples for some candidate i 's histogram, resulting in the empirical estimate \vec{r}_i . Then*

\vec{r}_i has ϵ_i -deviation with probability greater than $1 - \delta_i$ for

$$\epsilon_i = \sqrt{\frac{2|V_X|}{n_i} \log \frac{2}{\delta_i^{(1/|V_X|)}}}$$

That is, with probability $> 1 - \delta_i$, we have: $\|\vec{r}_i - \vec{r}_i^\|_1 < \epsilon_i$.*

PROOF. For $j \in [|V_X|]$, we use r_j to denote the number of occurrences of attribute value j among the n_i samples, and the normalized count \hat{r}_j is our estimate of \hat{r}_j^* , the true proportion of tuples having value j for attribute X . Note that we have omitted the candidate subscript i for clarity.

We need to introduce some machinery. Consider functions of the form $f : [|V_X|] \rightarrow \{+1, -1\}$. Let $\{f_m\}$ be the set of all such functions, where $m \in [2^{|V_X|}]$, since there are $2^{|V_X|}$ such functions. For any $m \in [2^{|V_X|}]$, consider the random variable

$$Y_m = \sum_{j=1}^{|V_X|} f_m(j)(\hat{r}_j - \hat{r}_j^*)$$

By linearity of expectation, it's clear that $\mathbb{E}[Y_m] = 0$, since $f_m(j)$ is constant and $\mathbb{E}[\hat{r}_j] = \hat{r}_j^*$ for each j . Since each \hat{r}_j is a function of the samples taken $\{s_k : 1 \leq k \leq n_i\}$, each Y_m is likewise uniquely determined from samples, so we can write $Y_m = g_m(s_1, \dots, s_{n_i})$, where each sample s_k is a random variable distributed according to $s_k \sim \vec{r}^*$. Note that the function g_m satisfies the Lipschitz property

$$|g_m(s_1, \dots, s_k, \dots, s_{n_i}) - g_m(s_1, \dots, s'_k, \dots, s_{n_i})| \leq \frac{2}{n_i}$$

for any $j \in [|V_X|]$ and s_1, \dots, s_{n_i} . For example, this will occur with equality if $f_m(s_k) = -f_m(s'_k)$; that is, if f_m assigns opposite signs to s_k and s'_k , then changing this single sample moves $1/n_i$ of the empirical mass in such a way that it does not get canceled out. We may therefore apply the method of bounded differences [43] to yield the following McDiarmid inequality:

$$\mathbb{P}(Y_m \geq \mathbb{E}[Y_m] + \epsilon_i) \leq \exp(-\epsilon_i^2 n_i / 2)$$

Recalling that $\mathbb{E}[Y_m] = 0$, this actually says that

$$\mathbb{P}(Y_m \geq \epsilon_i) \leq \exp(-\epsilon_i^2 n_i / 2)$$

This holds for any $m \in [2^{|V_X|}]$. Union bounding over all such m , we have that

$$\mathbb{P}(\exists m : Y_m \geq \epsilon_i) \leq 2^{|V_X|} \exp(-\epsilon_i^2 n_i / 2)$$

If this does not happen (i.e., for every Y_m , we have $Y_m < \epsilon_i$), then we have that $\|\vec{r}_i - \vec{r}_i^*\|_1 < \epsilon_i$, since for any attribute value j , $|\hat{r}_j - \hat{r}_j^*| = \max_{t_j \in \{+1, -1\}} t_j(\hat{r}_j - \hat{r}_j^*)$. But if $Y_m < \epsilon_i$ for all m , this means that we must have some m such that

$$\epsilon_i > \sum_j f_m(j)(\hat{r}_j - \hat{r}_j^*) = \sum_j |\hat{r}_j - \hat{r}_j^*| = \|\vec{r}_i - \vec{r}_i^*\|_1$$

As such $\mathbb{P}(\exists m : Y_m \geq \epsilon_i)$ is an upper bound on $\mathbb{P}(\|\vec{r}_i - \vec{r}_i^*\|_1 \geq \epsilon_i)$.

The desired result follows from noting that

$$\delta_i \leq 2^{|V_X|} \exp(-\epsilon_i^2 n_i / 2) \iff \epsilon_i \leq \sqrt{\frac{2|V_X|}{n_i} \log \frac{2}{\delta_i^{(1/|V_X|)}}} \quad \square$$

Optimality of the bound in Theorem 1. If we solve for n_i in Theorem 1, we see that it is necessary to have $n_i = \frac{2|V_X|}{\epsilon_i^2} \log \frac{2}{\delta_i^{(1/|V_X|)}}$.

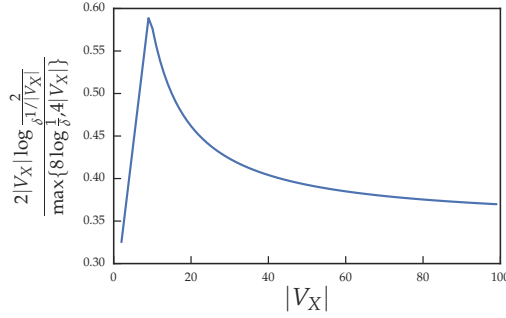


Figure 4: Ratio of bound in Theorem 1 to bound from [56].

That is, we require $\Omega\left(\frac{|V_X|}{\varepsilon_i^2}\right)$ samples before we can guarantee that the empirical discrete distribution \tilde{r}_i is no further than ε_i from the true discrete distribution r_i^* , with high probability. This matches the information theoretical lower bound noted in [10, 16, 21, 56].

Sensitivity and constant factors. In fact, our bound is not very sensitive to changes in δ_i due to the exponent $\frac{1}{|V_X|}$ in the log factor. We are only aware of one upper bound from prior work which matches the information theoretically-optimal lower bound asymptotically, which was given in Waggoner [56]. That bound, like ours, is optimal, but it has larger constant factors, which means that a system implemented on top of such theory will take more samples than really necessary to make a guarantee to the analyst, and thus take longer to answer queries. Figure 4 plots the ratio of our bound to the bound in [56] for $\delta = 0.01$ versus $|V_X|$ (the dependence on ε cancels), showing that our bound typically requires half or fewer samples to make the same level of guarantee. Our bound is tighter because of our indirect approach taken in the proof of Theorem 1: most work would start by showing that $\mathbb{E}[\|\tilde{r}_i - r_i^*\|_1]$ is small, and use this to show that $\|\tilde{r}_i - r_i^*\|_1$ is also small. We circumvent the first step via a novel construction specific to ℓ_1 distance.

3.5 Overall Proof of Correctness

We are now ready to prove the overall correctness of HistSim.

THEOREM 2. *The k histograms returned by Algorithm 1 satisfy Guarantees 1 and 2 with probability greater than $1 - \delta$.*

PROOF. At termination of Algorithm 1, a procedure which takes n_i uniform random samples for candidate i fails to satisfy ε_i -deviation with probability at most δ_i . Applying a union bound, the probability that *any* candidate i fails to satisfy ε_i -deviation is at most $\sum_i \delta_i = \delta^{upper} < \delta$. Thus, the probability that, for each i , candidate i has ε_i -deviation is greater than $1 - \delta$. Because the $\{\varepsilon_i\}$ were chosen to satisfy the separation and reconstruction guarantees, any algorithm which, for each i , takes n_i samples for a distance estimate of τ_i satisfies the separation and reconstruction guarantees with probability greater than $1 - \delta$. Algorithm 1 is such an algorithm (it terminates after taking n_i samples for each candidate i), so we are done. \square

Computational Complexity. Each iteration of Algorithm 1 runs in time $\mathcal{O}(|V_Z| \cdot |V_X| + |V_Z| \log |V_Z|)$. For each candidate i , we update \tilde{r}_i and τ_i based on new samples, which takes $\mathcal{O}(|V_Z| \cdot |V_X|)$ across all candidates. Then, to choose the split point s and the deviations $\{\varepsilon_i\}$, we must sort the candidates, which is $\mathcal{O}(|V_Z| \log |V_Z|)$. Alternatively, we could perform a Quick Select [20] to find the boundary between the top- k and non-top- k for a time of $\mathcal{O}(|V_Z|)$, bringing overall complexity down to $\mathcal{O}(|V_Z| \cdot |V_X|)$, but our actual implementation uses the sort.

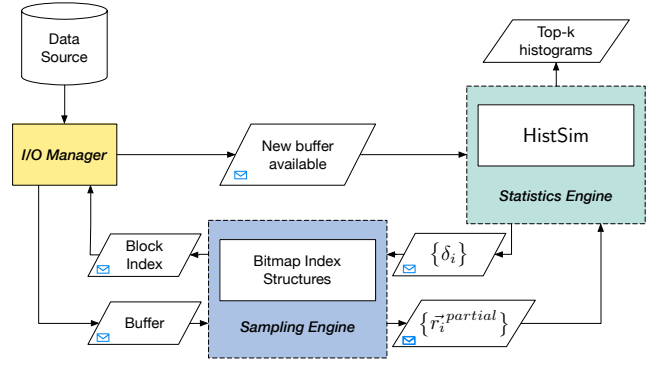


Figure 5: FastMatch system architecture

4. THE FASTMATCH SYSTEM

This section describes FastMatch, which implements the HistSim algorithm within the context of a real system. We start by presenting the high-level components of FastMatch. We then describe the challenges we faced while implementing FastMatch and describe how the components interact to alleviate those challenges, while still satisfying Guarantees Guarantee 1 and Guarantee 2.

4.1 FastMatch Components

FastMatch has three key components: the I/O Manager, the Sampling Engine, and the Statistics engine. We describe each of them in turn; Figure 5 provides an architecture diagram—we will revisit the interactions within the diagram at the end of the section.

I/O Manager. In FastMatch, requests for I/O are serviced at the granularity of *blocks*. We set the block size to 4 KiB, which matches the sector sizes for typical storage devices. The I/O manager simply services requests for blocks in a synchronous fashion. Given the location of some block, it synchronously reads the block at that location into a memory buffer.

Sampling Engine. The sampling engine is responsible for deciding which blocks to sample. It uses bitmap index structures (described below) in order to determine the types of samples located at a given block. Given the current state of the system, it prioritizes certain candidates over others for sampling.

Statistics Engine. The statistics engine implements most of the logic in the HistSim algorithm. The only substantial difference between the actual code and the pseudocode presented in Algorithm 1 is that the statistics engine does not actually perform any sampling, instead communicating with the sampling engine to facilitate sampling. The reason for separating these components will be made clear later on.

Bitmap Index Structures. FastMatch runs on top of a bitmap-based online sampling system, as in prior work [7, 36, 35, 50]. These papers have demonstrated that bitmap indexes [15] are effective in supporting sampling for incremental or early termination of visualization generation. Within FastMatch, bitmap indexes help the sampling engine determine whether a given block contains samples for a given candidate. For each attribute A , and each attribute value A_v , we store a bitmap, where a ‘0’ at position p indicates that the corresponding block at position p contains no tuples with attribute value A_v , and a ‘1’ indicates that block p contains one or more tuples with attribute value A_v . Candidate visualizations are generated by attribute values (or a predicate of ANDs and ORs over attribute values; see Appendix A), so these bitmaps allow the sampling engine to rapidly test whether a block contains tuples for a given candidate histogram. Bitmap indexes are amenable to significant compression [58, 59], and since we are further only requiring

a single bit per block per attribute value, our storage requirements are orders-of-magnitude cheaper than past work that requires a bit per tuple [7, 35, 50].

4.2 Implementation Challenges

So far, we have designed HistSim without worrying about how sampling actually takes place, with an implicit assumption that there is no overhead to taking samples randomly across various candidates. While implementing HistSim within the context of FastMatch, we faced several non-trivial challenges, outlined below:

- **Challenge 1: Random sampling at odds with performance characteristics of storage media.** The cost to fetch data is locality-dependent when dealing with real storage devices. Even if the data is stored in-memory, tuples (i.e., samples) that are spatially closer to a given tuple may be cheaper to fetch, since they may already be present in CPU cache.
- **Challenge 2: Non-uniform cost/benefit of different candidates.** Tuples for some candidate histograms can be over-represented in the data and therefore take less time to sample compared to underrepresented candidates. At the same time, the benefit of sampling tuples corresponding to different candidate histograms is non-uniform: for example, those histograms which are “far” from the target distribution are less useful (in terms of getting HistSim to terminate quickly) than those for which HistSim chooses small values for ε_i .
- **Challenge 3: Assessing benefit to candidates depends on data seen so far.** The “best” choice of which tuples to sample for getting HistSim to terminate quickly can be most accurately estimated from *all* the data seen so far, including the most recent data. However, computing this estimate after processing every tuple and blocking I/O until the “best” decision can be made is prohibitively expensive.

We now describe our approaches to tackling these three challenges.

Challenge 1: Randomness via Data Layout

To maximize performance benefits from locality, we randomly permute the tuples of our dataset as a preprocessing step, and to “sample” we may then simply perform a linear scan of the shuffled data starting from any point. Although the theory we developed in Section 3 was for sampling with-replacement, it still holds now that we are sampling without replacement — this can be seen by noting that the Lipschitz condition from Theorem 1 becomes even tighter in the without-replacement regime, so that the with-replacement ε_i will be larger than its without-replacement counterpart. This approach of randomly permuting upfront is not new, and is adopted by other approximate query processing systems [60, 49, 62].

Challenge 2: Block Choice Policies

Our next challenge is that the non-uniform cost (i.e., time) and benefit of samples for each candidate histogram makes it difficult to decide which blocks to read. If either cost or benefit were uniform across candidates, matters would be simplified significantly: if cost were uniform, we could simply read in the blocks with the most beneficial candidates; if benefit were uniform, we could simply read in the lowest cost blocks (for example, those closest spatially to the current read position). To address these concerns, we developed a simple policy which we found worked well in practice for getting HistSim to terminate quickly.

AnyActive block selection policy. Recall that each iteration of HistSim computes a set of deviations $\{\delta_i\}$, where each δ_i is an upper bound on the probability that candidate i fails to have ε_i -deviation. Note that if every δ_i satisfied $\delta_i \leq \frac{\delta}{|V_Z|}$, then HistSim

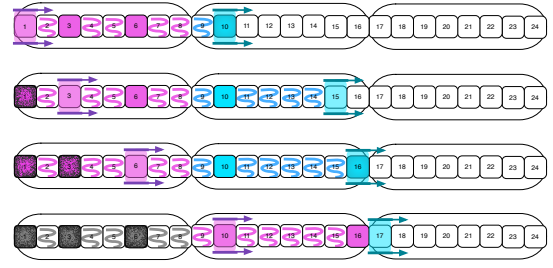


Figure 6: While the I/O manager processes magenta blocks, the sampling engine selects blue blocks ahead of time, using lookahead. Blocks with solid color = read, blocks with squiggles = skip.

would be in a state where it can safely terminate. Those candidates for whom $\delta_i > \frac{\delta}{|V_Z|}$ we dub *active candidates*, and we employ a very simple block selection policy, dubbed the AnyActive block selection policy, which is to *only read blocks which contain at least one tuple corresponding to some active candidate*. The bitmap indexes employed by FastMatch allow it to rapidly test whether a block contains tuples for a given candidate visualization, and thus to rapidly apply the AnyActive block selection policy. Overall, our approach is as follows: we read blocks in sequence, and if blocks satisfy our AnyActive criterion, then we read all of the tuples in that block, else, we skip that block. In actuality, our approach is a bit more complicated, as we will see below.

A naive variant of this policy is presented in Algorithm 2, for which we describe improvements below.

Challenge 3: Asynchronous Block Selection

From the previous discussion, the sampling engine employs an AnyActive block selection policy when deciding which blocks to process. Ideally, the $\{\delta_i\}$ used to assign active status to candidates should be computed from the freshest possible data available to HistSim. Unfortunately, this requirement is at odds with real system characteristics. Employing it exactly implies running an iteration of HistSim to compute fresh $\{\delta_i\}$ after every block is processed. This causes two intertwined problems.

- **Problem 1:** The sampling engine is idle while it waits for the freshest $\{\delta_i\}$ from the statistics engine, *every single time it decides whether to process a block*.
- **Problem 2:** The I/O manager is idle while it waits for the sampling engine to select a block for reading.

Unblocking the Sampling Engine. Note that a solution to the first problem is a prerequisite for a solution to the second problem—blocking the sampling engine transitively blocks the I/O manager. As such, we focus on it first. To solve this problem, we decouple the computation performed in the statistics engine from the decisions made by the sampling engine. To do so, the statistics engine runs in a separate thread, and communicates with the sampling engine via shared-memory messages.

Each time the statistics engine performs a HistSim iteration, it posts the $\{\delta_i\}$ available to the sampling engine, which runs independently. This way, the sampling engine need not idle while it waits for new data, but can simply use the freshest $\{\delta_i\}$ available when making decisions with the AnyActive selection policy. The sampling engine also “messages” the statistics engine in order make samples available: for each candidate i , the sampling engine stores group counts for candidate i in a temporary location $\vec{r}_i^{\text{partial}}$. The statistics engine then performs the following update at the beginning of each iteration:

$$\vec{r}_i \leftarrow \vec{r}_i + \vec{r}_i^{\text{partial}} \quad \vec{r}_i^{\text{partial}} \leftarrow \vec{0}$$

Algorithm 2: Naive AnyActive block processing

Input : active candidate set A , block index i
Output : A value indicating whether to :read or :skip block i

```

1 for cand  $\in A$  do
  // cache inefficient index lookup
  // evicts bits from previous candidate's bitmap index
2 if cand.index_lookup(i) then
3   return :read;
4 end
5 end
6 return :skip;

```

For improved cache performance, it only performs the update when $\vec{r}_i^{\text{partial}} \neq 0$; otherwise, it performs no writes in order to leave $\vec{r}_i^{\text{partial}}$ in a shared state with the sampling thread's CPU. For thread safety, the $\{\vec{r}_i^{\text{partial}}\}$ are protected with simple spinlocks, which avoid putting threads to sleep. This is acceptable since the critical section is very small.

Unblocking the I/O Manager. Solving the second problem turned out to be more difficult and amounted to optimizing the time it takes for the sampling engine to perform AnyActive block selection. To do so, we needed to relax the requirement that the sampling thread employ AnyActive with the freshest $\{\delta_i\}$ available to it. Instead, given a fresh set of $\{\delta_i\}$, it “looks ahead” and marks an entire batch of blocks for either reading or skipping, and communicates this with the I/O manager. The batch size, or the *lookahead* amount, is a parameter we have to set, and offers a trade-off between freshness of $\{\delta_i\}$ used for AnyActive and degree to which the I/O manager must idle while waiting for instructions on which block to read next. We evaluate the impact of this parameter in our experimental section. The lookahead process is depicted in Figure 6 for a value of *lookahead* = 8. While the I/O manager processes a previously marked batch of magenta-colored lookahead blocks, the sampling engine's lookahead thread marks the next batch in blue. It waits to mark the next batch until the I/O manager “catches up”.

Employing *lookahead* allows us to prevent two bottlenecks. First, because the sampling engine need not wait for the freshest $\{\delta_i\}$ from the statistics engine, it also does not need to wait for the I/O manager to complete requests, since it no longer needs to wait for the freshest data from the I/O manager to eventually make its way to the statistics engine.

The second bottleneck prevented by *lookahead* is more subtle. To illustrate it, consider the pseudocode in Algorithm 2, implementing the AnyActive block policy. The AnyActive block policy algorithm works by considering each candidate in turn, and querying a bitmap index for that candidate to determine whether the current block contains tuples corresponding to that candidate. Querying a bitmap actually brings in surrounding bits into the cache of the CPU performing the query, and evicts whatever was previously in the cache line. If blocks are processed individually, then only a single bit in the bitmap is used each time a portion is brought into cache. This is quite wasteful and turns out to hurt performance significantly as we will see in the experiments. Instead, applying AnyActive selection to lookahead-size chunks instead of individual blocks is a better approach. This simply adds an extra inner loop to the procedure shown in Algorithm 2 (depicted in Algorithm 3). This approach has much better cache performance, since it uses an entire cache-line's worth of bits while employing AnyActive.

Algorithm 3: AnyActive block selection with lookahead

Input : lookahead amount, start block, active candidate set A
Output : An array *mark* indicating whether to :read or :skip blocks

```

// Initialization
1 mark[i]  $\leftarrow$  :skip for  $0 \leq i < \text{lookahead}$ ;
2 for cand  $\in A$  do
3   for  $0 \leq i < \text{lookahead}$  do
4     if mark[i] == :read then
5       continue;
6     else if cand.index_lookup(start + i) then
7       mark[i]  $\leftarrow$  :read;
8     end
9   end
10 end
11 return mark

```

We verify in our experiments that these optimizations allow FastMatch to terminate more quickly via AnyActive block selection with *fresh-enough* $\{\delta_i\}$ without significantly slowing any single component of the system.

4.3 System Architecture

FastMatch is implemented within a few thousand lines of C++. It uses `pthreads` [46] for its threading implementation and to pin threads to cores via thread affinities. We use FastMatch in a row-store mode in order to obviate any benefits from column-stored data and better test the components described in this section.

We can now complete our description of Figure 5. When the I/O manager receives a request for a block at a particular block index from the sampling engine (via the “block index” message), it eventually returns a buffer containing the data at this block to the sampling engine (via the “buffer” message). It also posts a “new buffer available” message to the statistics engine, which then knows it may accept a message of updated candidate histogram counts ($\vec{r}_i^{\text{partial}}$) from the sampling engine. After running a HistSim iteration, the statistics engine posts a message of updated $\{\delta_i\}$ used by the sampling engine for block selection.

Additional Notes on the Sampling Engine. The sampling engine actually uses two threads: one which employs the AnyActive policy to mark batches of *lookahead* blocks for either reading or skipping, and one which processes raw buffers delivered by the I/O manager into $\vec{r}_i^{\text{partial}}$ for eventual delivery to the statistics engine.

5. EXPERIMENTAL EVALUATION

The goal of our experimental evaluation is to test the accuracy and runtime of FastMatch against other approximate and exact approaches on a diverse set of real datasets and queries. Furthermore, we want to validate the design decisions that we made for FastMatch in Section 4 and evaluate their impact.

5.1 Datasets and Queries

We evaluate FastMatch on publicly available real-world datasets summarized in Table 2—spanning flight records [1], taxi trips [2], and police road stops in the state of Washington [3]. The replication value indicates how many times each dataset was replicated to

Dataset	Size	#Tuples	#Attributes	Replications
FLIGHTS	32 GiB	604 million	7	5×
TAXI	36 GiB	677 million	7	4×
POLICE	29 GiB	382 million	10	72×

Table 2: Descriptions of Datasets

Dataset	Query	Z ($ V_Z $)	X ($ V_X $)	k	target
FLIGHTS	q ₁	Origin (161)	DepartureHour (24)	10	Chicago ORD
	q ₂	Origin (161)	DepartureHour (24)	10	Appleton ATW
	q ₃	Origin (161)	DayOfWeek (7)	5	[0.25, 0.125, 0.125, 0.125, 0.125, 0.125]
	q ₄	Origin (161)	Dest (161)	10	closest candidate to uniform
TAXI	q ₁	Location (7548)	HourOfDay (24)	10	closest candidate to uniform
	q ₂	Location (7548)	MonthOfYear (12)	10	closest candidate to uniform
POLICE	q ₁	RoadID (191)	ContrabandFound (2)	10	closest candidate to uniform
	q ₂	RoadID (191)	OfficerRace (5)	10	closest candidate to uniform
	q ₃	Violation (2110)	DriverGender (2)	5	closest candidate to uniform

Table 3: Summary of queries

create a larger dataset. In preprocessing these datasets, we eliminated rows with “N/A” values for certain columns; and to ensure that there is an adequate number of samples across candidates, we pruned tuples with attribute values that appear fewer than 2000 times in the data (such tuples constituted fewer than 1% of the data, for every dataset).

FLIGHTS Dataset. Our FLIGHTS dataset, representing delays measured for flights at 161 major airports from 1987 up to 2008, is available at [1]; We used 7 attributes (for origin / destination airports, departure / arrival delays, day of week, day of month, and departure hour).

TAXI Dataset. Our TAXI dataset summarizes all Yellow Cab trips in New York in 2013 [2]. The subset of data we used corresponds with the urls ending in “yellow_tripdata_2013” in the file raw_data_urls.txt. We extracted some time-based discrete attributes, two attributes based on passenger count, and one attribute based on area, for 7 columns total. In particular, the “Location” attribute was generated by binning the pickup location into regions of 0.01 longitude by 0.01 latitude. As with our FLIGHTS data, we discarded rows with missing values, as well as rows with outlier longitude or latitude values (which did not correspond to real locations).

POLICE Dataset. Our POLICE dataset summarizes more than 8 million police road stops in Washington state [3]. We extracted attributes for county, two gender attributes, two race attributes, road number, violation type, stop outcome, whether a search was conducted, and whether contraband was found, for 10 attributes total.

Queries and Query Format. We evaluate several queries on each dataset, whose templates are summarized in Table 3. We had four queries on FLIGHTS, FLIGHTS-q1-q4, two on TAXI, TAXI-q1-q2, and three on POLICE, POLICE-q1-q3. For simplicity, in all queries we test the x-axis is generated by grouping over a single attribute (denoted by “X” in Table 3), and the different candidates are likewise generated by grouping over a single (different) attribute (signified by “Z”). For each query, the visual target was chosen to correspond with the closest distribution (under ℓ_1) to uniform, out of all histograms generated via the query’s template, except for q1, q2, and q3 of FLIGHTS. Our queries spanned a number of interesting dimensions: (i) *frequently-appearing top-k candidates*: FLIGHTS-q1, POLICE-q1 and q2, (ii) *rarely-appearing top-k candidates*: FLIGHTS-q2 and q3, (iii) *high-cardinality candidate attribute Z*: TAXI-q1 and q2 ($|V_Z| = 7548$), POLICE-q3 ($|V_Z| = 2110$), and (iv): *high-cardinality grouping attribute X*: FLIGHTS-q4 ($|V_X| = |V_Z| = 161$).

5.2 Experimental Setup

Approaches. We compare FastMatch against a number of less sophisticated approaches that provide the same guarantee as FastMatch. Except for Scan, they are all parametrized by ϵ and δ and satisfy Guarantees 1 and 2 with probability greater than $1 - \delta$.

- **SyncMatch(ϵ, δ).** This approach uses FastMatch, but the AnyActive block selection policy is applied without lookahead, synchronously and for each individual block. *By comparing this method with FastMatch, we quantify how much benefit we may ascribe to the lookahead technique.*
- **ScanMatch(ϵ, δ).** This approach uses FastMatch, but without the AnyActive block selection policy. Instead, no blocks are pruned: it scans through each block in a sequential fashion until the statistics engine reports that HistSim’s termination criterion holds. *By comparing this method with SyncMatch, we quantify how much benefit we may ascribe to AnyActive block selection.*
- **SlowMatch(ϵ, δ).** This approach uses ScanMatch, but with a termination criterion that requires more samples. Specifically, the statistics engine runs a variant of HistSim that generates $1 - \frac{\delta}{|V_Z|}$ confidence intervals around each candidate, and then tests whether (a) any of the top-k estimated candidates have intervals wider than ϵ , or (b) any of the top-k overlap any of the non-top-k by an amount more than ϵ . If either (a) or (b) hold, the algorithm does not terminate. Note that this is equivalent to running HistSim until $\max_i \{\delta_i\} \leq \frac{\delta}{|V_Z|}$ instead of the more intelligent termination criterion $\sum_i \delta_i \leq \delta$. *By comparing this method with ScanMatch, we quantify how much benefit we may ascribe to HistSim’s intelligent termination criterion.*
- **Scan.** This approach is a simple heap scan over the entire dataset and always returns correct results, trivially satisfying Guarantees 1 and 2. *By comparing Scan with our above approximate approaches, we quantify how much benefit we may ascribe to the use of approximation.*

Environment. Experiments were run on single Intel Xeon E5-2630 node with 125 GiB of RAM and with 8 physical cores (16 logical) each running at 2.40 GHz, although we use at most 4 logical cores to run FastMatch components. The Level 1, Level 2, and Level 3 CPU cache sizes are, respectively: 512 KiB, 2048 KiB, and 20480 KiB. We ran Linux with kernel version 2.6.32. We report results for data stored in-memory (using the tmpfs file system), since the cost of main memory has decreased to the point that most interactive workloads can be performed entirely in-core.

To ensure sufficient randomness, each run of FastMatch or any other approximate approach was started from a random position in the shuffled data (selected using a Mersenne Twister [42] pseudo-random generator seeded with the current time). We found wall clock time to be very stable for all approaches, so any times are reported as the average of 5 runs for all methods. Experiments related to accuracy had higher variance; we report any accuracy-related metrics averaged across 30 runs for all methods (excepting Scan). Where applicable, we used default settings of $\delta = 0.01$, $\epsilon = 0.06$, and lookahead = 512.

5.3 Metrics

Query	Avg Speedup over Scan (raw time in (s))				
	Scan time (s)	SlowMatch	ScanMatch	SyncMatch	FastMatch
FLIGHTS-q1	18.313	11.787× (1.554)	14.133× (1.296)	18.215× (1.005)	21.574× (0.849)
FLIGHTS-q2	18.185	1.336× (13.614)	1.654× (10.994)	3.663× (4.964)	15.128× (1.202)
FLIGHTS-q3	16.112	0.995× (16.191)	1.417× (11.370)	2.244× (7.181)	7.347× (2.193)
FLIGHTS-q4	25.983	27.909× (0.931)	30.670× (0.847)	38.967× (0.667)	39.803× (0.653)
TAXI-q1	17.621	0.992× (17.761)	1.343× (13.118)	0.144× (122.574)	12.790× (1.378)
TAXI-q2	16.982	1.001× (16.958)	1.278× (13.283)	0.137× (123.860)	7.338× (2.314)
POLICE-q1	10.220	9.660× (1.058)	16.716× (0.611)	15.695× (0.651)	22.329× (0.458)
POLICE-q2	10.181	30.701× (0.332)	46.829× (0.217)	62.611× (0.163)	99.903× (0.102)
POLICE-q3	10.134	26.796× (0.378)	44.921× (0.226)	18.181× (0.557)	136.509× (0.074)

Table 4: Summary of average query speedups and latencies

We use several metrics to compare FastMatch against our baselines in order to test two hypotheses: one, that FastMatch does indeed provide accurate answers, and two, that the system architecture developed in Section 4 does indeed allow for earlier termination while satisfying the separation and reconstruction guarantees.

Wall-Clock Time. Our primary metric evaluates the end-to-end time of our approximate approaches that are variants of FastMatch, as well as a scan-based baseline.

Satisfaction of Guarantees Guarantee 1 and Guarantee 2. Our δ parameter ($\delta = 0.01$), serves as an upper bound on the probability that either of these guarantees are violated. If this bound were tight, we would expect to see about one run in every hundred fail to satisfy our guarantees. We therefore count the number of times our guarantees are violated and compare it against the total number of queries performed.

Total Relative Error in Visual Distance. In some situations, there may be several candidate histograms that are quite close to the analyst-supplied target, and choosing any one of them to be among the k returned to the analyst would be a good choice. We define the *total relative error in visual distance* (denoted by Δ_d) between the k candidates returned by FastMatch and the true k closest visualizations as follows:

$$\Delta_d(M, M^*, \vec{Q}) = \frac{\sum_{i \in M} d(\vec{r}_i, \vec{Q}) - \sum_{j \in M^*} d(\vec{r}_j^*, \vec{Q})}{\sum_{j \in M^*} d(\vec{r}_j^*, \vec{Q})}$$

We always have that $\Delta_d \geq 0$, with smaller values corresponding to higher-quality results.

5.4 Empirical Results

Speedups and Error of FastMatch over others.

Summary. All FastMatch variants we tested show significant speedups over Scan for at least one query, but only FastMatch shows consistently excellent performance, typically beating other approaches and bringing latencies for all queries near interactive levels; with an overall speedup ranging between **7× and 136×** over Scan. Further, the output of FastMatch **and all approximate variants satisfied Guarantees 1 and 2 across all runs for all queries.**

Average run times of FastMatch and other approaches, for all queries as well as speedups over Scan, are summarized in Table 4. We used default settings for all runs, with the exception of those for query FLIGHTS-q4, which we report at $\varepsilon = 0.07$ (for reasons explained later). The reported speedups are the ratio of the average wall time of Scan with the average wall time of each approach considered. Scan was generally slower than approximate approaches because it had to examine all the data. Then, we typically observed that SlowMatch took longer than ScanMatch due to its worse termination criterion, which in turn generally took longer than SyncMatch because it was not able to employ AnyActive block selection. FastMatch had even better performance

than SyncMatch, thanks to lookahead. Overall, we observed that each of FastMatch’s key innovations: the termination criterion, the block selection, and lookahead, all led to substantial performance improvements, with an overall speedup of up to **136×** over Scan.

There were a few notable cases that displayed unusual differences in performance. In the case of a large number of candidates, represented by the TAXI queries, all candidates are relatively infrequent (since there are many of them) and FastMatch shows greatly improved performance over ScanMatch and SlowMatch. SyncMatch, on the other hand, performs extremely poorly due to poor cache utilization and takes nearly $7\times$ longer than a simple non-approximate Scan. In this case, the lookahead technique of FastMatch is necessary to reap the benefits of AnyActive block selection.

The top- k candidates were relatively rare compared to others for queries FLIGHTS-q2 and FLIGHTS-q3. In these cases, AnyActive block selection via SyncMatch resulted in significant speedups over other approximate variants due to more aggressive pruning of blocks. For example, SyncMatch was about $2.2\times$ faster than ScanMatch on FLIGHTS-q2 and $1.6\times$ faster on FLIGHTS-q3. FastMatch resulted in even more speedups over SyncMatch, about $4.1\times$ on FLIGHTS-q2 and $3.3\times$ on FLIGHTS-q3.

Additionally, we found that the output of FastMatch *and all approximate variants satisfied Guarantees 1 and 2 across all runs for all queries*. This suggests that the parameter δ may be a loose upper bound for the actual failure probability of FastMatch.

Effect of varying ε .

Summary. In almost all cases, increasing the tolerance parameter ε leads to reduced runtime and accuracy, but **on average, Δ_d was never more than 6% larger than optimal for any query, even for the largest values of ε used.**

Figure 7 Figure 8 depict the effect of varying ε on the wall clock time and on Δ_d , respectively, using $\delta = 0.01$ and lookahead = 512, averaged over 5 runs for wall clock time and 30 runs for Δ_d for each value of ε . Because of the extremely poor performance of SyncMatch on the TAXI queries, we omit it from both figures.

In general, as we increased ε , wall clock time decreased and Δ_d increased. In some cases, SlowMatch and ScanMatch latencies matched that of Scan until we made ε large enough. For SlowMatch, this usually happened when the method failed to pass the HistSim safe-termination test and ended up reading all the data. For ScanMatch, this sometimes happened when it needed more refined estimates of the (relatively infrequent) top- k candidates, which it achieved by scanning most of the data, picking up lots of superfluous (in terms of achieving safe termination) tuples along the way.

We note that for $\varepsilon = 0.06$, we have omitted the data point for SyncMatch on query FLIGHTS-q4 due to the presence of several outlying runs. For this query at this value of ε , we observed a subset of the runs take significantly longer ($\approx 6s$) at some starting points, consistently. Due to this, for the FLIGHTS-q4 entries in Table 4, we report results for all approaches for $\varepsilon = 0.07$ instead of $\varepsilon = 0.06$.

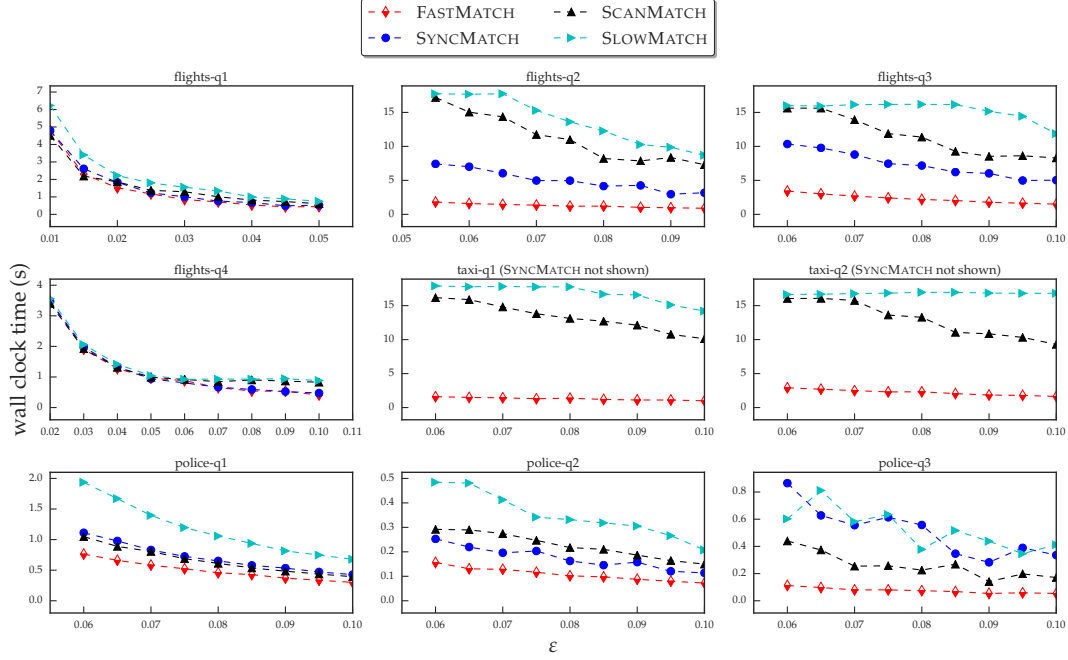


Figure 7: Effect of ε on query latency

We believe that this is due poor cache performance of SyncMatch and inconsistent ability to reduce the number of active candidates quickly at $\varepsilon = 0.06$, for different starting positions.

Effect of varying lookahead.

Summary. When the number of candidates $|V_Z|$ is not large, performance is relatively stable as lookahead varies. For large $|V_Z|$, a larger value of lookahead helps performance, but is not crucial.

For most queries, we found that latency was relatively robust to changes in lookahead. Figure 9 depicts this effect. The exception to this was the TAXI queries, for which larger lookahead values led to increased utilization at all levels of CPU cache. The performance gains were minor, however; we found the default value of 512 to be acceptable in all circumstances.

Effect of varying δ . In general, we found that both wall clock time and accuracy (in terms of Δ_d or satisfaction of Guarantees 1 and 2) are more-or-less constant in δ , with very slight decreases in query latency and accuracy. We believe this behavior is inherited from our bound in Theorem 1, which is not sensitive to changes in δ . Figures 10 and 11 show the effect of varying δ on wall clock time and accuracy, respectively.

6. RELATED WORK

We now briefly cover work that is related to FastMatch from a number of different areas.

Approximate Query Processing. There are two forms of approximate query processing—offline and online. Offline approximate query processing involves computing a set of samples offline, and then using these samples online when queries arrive e.g., [31, 17, 4, 8, 6]. Systems that implement offline approximate query processing include BlinkDB [6] and Aqua [5]. These techniques crucially rely on the availability of a workload. On the other hand, online approximate query processing, e.g., [27, 28, 39], performs sampling on-the-fly, typically using an index to facilitate the identification of appropriate samples. Our work falls into the latter category; however, none of the prior work has addressed a similar problem of identifying relevant visualizations given a query.

Top-K Query Processing. There is a vast body of work on top-k query processing [29]. Most of this work relies on exact answers, as opposed to approximate answers, and has different objectives. As an example, Bruno et al. [13] exploit statistics maintained by a RDBMS in order to quickly find top- k tuples matching user-specified attribute values. Some work tries to bridge the gap between top-k query processing and uncertain query processing [53, 51], but does not need to deal with the concerns of where and when to sample to return answers quickly, but approximately.

Scalable Visualizations. There has been some limited work on scalable approximate visualizations, targeting the generation of a single visualization as fast as possible, while preserving certain properties [35, 47, 50]. In our setting, the space of sampling is much larger—as a result the problem is more complex. Furthermore, the objectives are very different.

Work on SeeDB [55] addresses a similar problem—it attempts to find “interesting” visualization axes, such that the distance between two subsets of data on those axes is as large as possible. Thus, like our paper, this paper also considers distances between a collection of many pairs of visualizations. However, the solution described is a heuristic and does not provide any accuracy guarantees.

Fisher et al. [23] explores the impact of approximate visualizations on users, adopting an online-aggregation-like [27] scheme. As such, these papers show that users are able to interpret approximate visualizations correctly and make decisions using them. Some work uses pre-materialization for the purpose of displaying visualizations quickly [34, 37, 41]; however, these techniques rely on an in-memory data cube, which is infeasible for large datasets.

We additionally covered other work on scalable visualization via approximation [22, 44, 33, 47, 61] in Section 1.

Histogram Estimation for Query Optimization. A number of related papers [18, 30, 32] are concerned with the problem of sampling for histogram estimation, usually for estimating attribute value selectivities [38] and query size estimation (see [19] for a recent example). While some of the theoretical tools used in analysis are similar to those employed in this work, the problem is fundamentally different, in that the aforementioned line of work is concerned

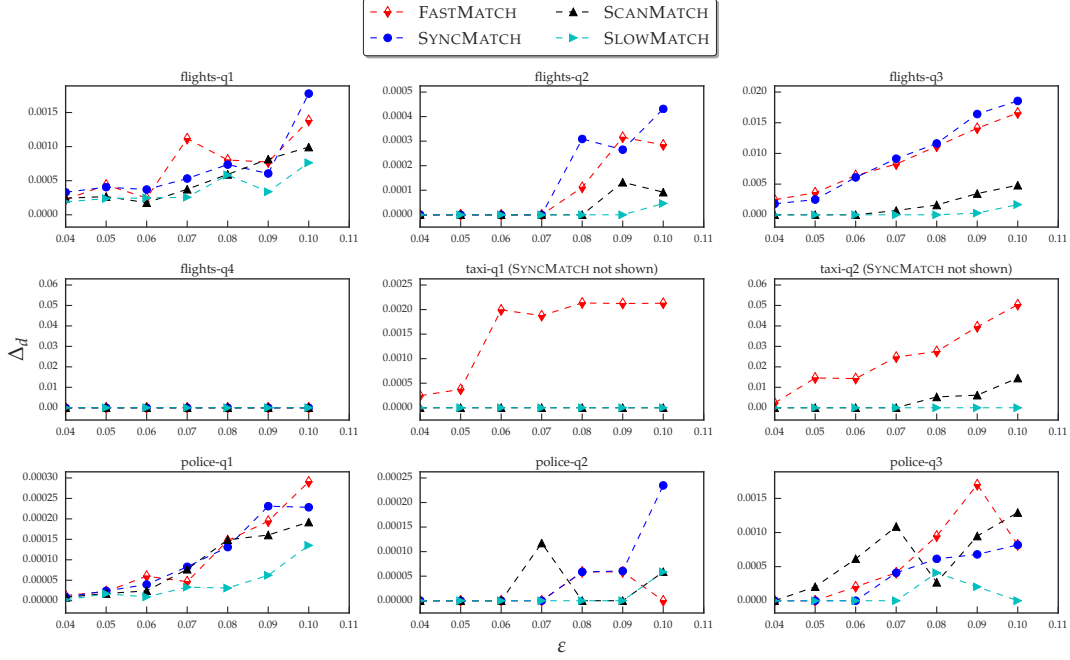


Figure 8: Effect of ε on Δ_d

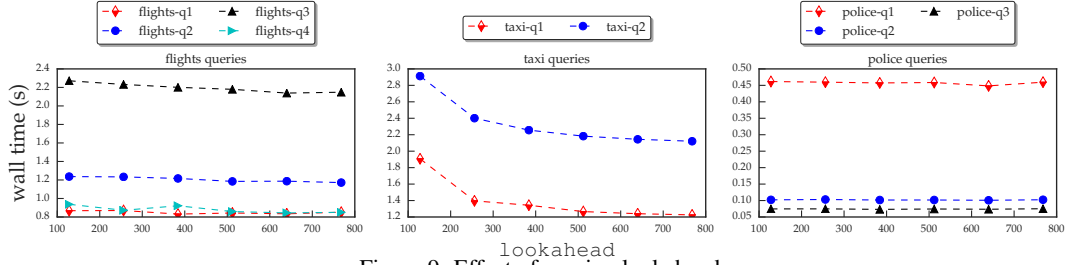


Figure 9: Effect of varying lookahead

with estimating one histogram per table or view for query optimization purposes with low error, while we are concerned with comparing histograms to rapidly identify those that are visually similar to a specific target.

Sublinear Time Algorithms. HistSim belongs to the family of sublinear time algorithms, since the algorithm described requires a number of samples that is generally sublinear in the size of the dataset. The most relevant works [10, 16, 56] fall under the setting of distribution learning and analysis of *property testers* for whether distributions are close under ℓ_1 distance. Although Chan et al. [16] develop optimal bounds for the problem of testing whether distributions are ε -close in the ℓ_1 metric, property testers can only say when two distributions p and q are equal or ε -far, and cannot handle $\|p - q\|_1 < \varepsilon$ for $p \neq q$, a necessary component of this work.

7. CONCLUSIONS AND FUTURE WORK

We developed sampling-based strategies for rapidly identifying the top- k histograms that are closest to a target. We designed a general algorithm, HistSim, that provides a principled framework to facilitate this search, with theoretical guarantees. We showed how the systems-level optimizations present in our FastMatch architecture are crucial for achieving near-interactive latencies consistently, leading to speedups ranging from $7\times$ to over $100\times$ over baselines. While this work suggests several possible avenues for further exploration, we are particularly interested in exploring the impact of our systems architecture in supporting general interactive analysis.

8. REFERENCES

- [1] Flight Records. <http://stat-computing.org/dataexpo/2009/the-data.html>, 2009.
- [2] NYC Taxi Trip Records. <https://github.com/toddwschneider/nyc-taxi-data/>, 2015.
- [3] WA Police Stop Records. <https://stacks.stanford.edu/file/druid:py883nd2578/WA-clean.csv.gz>, 2017.
- [4] S. Acharya, P. B. Gibbons, and V. Poosala. Congressional samples for approximate answering of group-by queries. In *ACM SIGMOD Record*, volume 29, pages 487–498. ACM, 2000.
- [5] S. Acharya, P. B. Gibbons, V. Poosala, and S. Ramaswamy. The aqua approximate query answering system. In *ACM Sigmod Record*, volume 28, pages 574–576. ACM, 1999.
- [6] S. Agarwal, B. Mozafari, A. Panda, H. Milner, S. Madden, and I. Stoica. Blinkdb: Queries with bounded errors and bounded response times on very large data. In *EuroSys*, pages 29–42, New York, NY, USA, 2013. ACM.
- [7] D. Alabi and E. Wu. Pfunk-h: approximate query processing using perceptual models. In *HILDA@ SIGMOD*, page 10, 2016.
- [8] N. Alon, Y. Matias, and M. Szegedy. The space complexity of approximating the frequency moments. In *STOC*, pages 20–29. ACM, 1996.

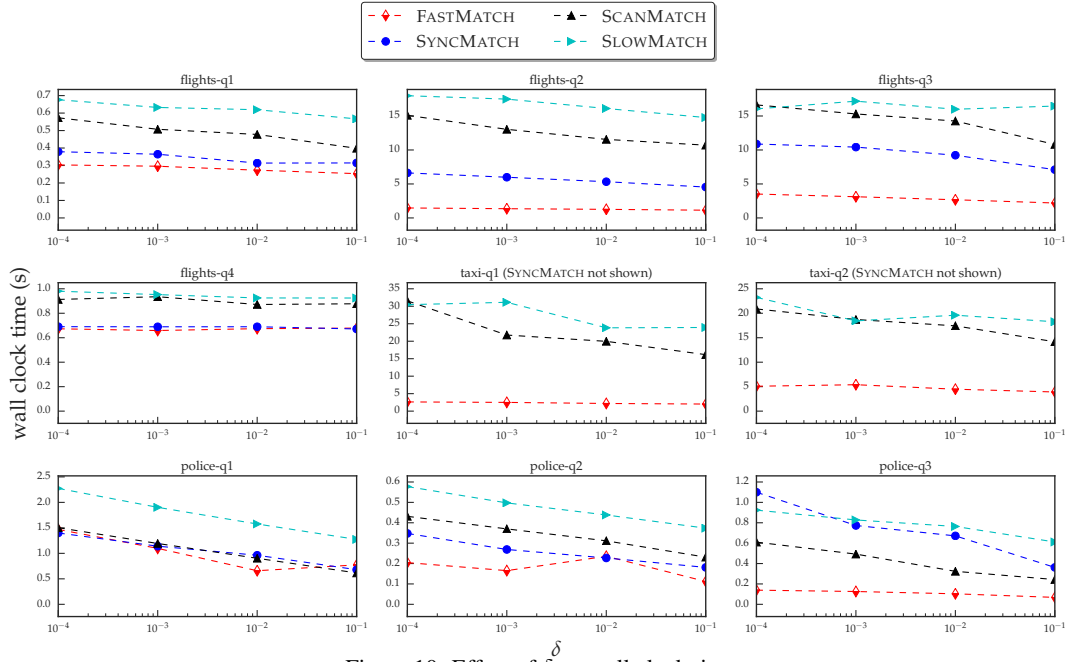


Figure 10: Effect of δ on wall clock time

- [9] B. Babcock, S. Chaudhuri, and G. Das. Dynamic sample selection for approximate query processing. In *SIGMOD*, New York, New York, USA, 2003.
- [10] T. Batu, L. Fortnow, R. Rubinfeld, W. D. Smith, and P. White. Testing that distributions are close. In *FOCS*, 2000.
- [11] J. T. Behrens. Principles and procedures of exploratory data analysis. *Psychological Methods*, 2(2):131, 1997.
- [12] M. Bostock, V. Ogievetsky, and J. Heer. D³ data-driven documents. *IEEE TVCG*, 17(12):2301–2309, 2011.
- [13] N. Bruno, S. Chaudhuri, and L. Gravano. Top-k selection queries over relational databases: Mapping strategies and performance evaluation. *ACM TODS*, 27(2):153–187, June 2002.
- [14] K. Chakrabarti, M. Garofalakis, R. Rastogi, and K. Shim. Approximate query processing using wavelets. *The VLDB Journal*, 10(2-3):199–223, Sept. 2001.
- [15] C.-Y. Chan and Y. E. Ioannidis. Bitmap index design and evaluation. In *ACM SIGMOD Record*, volume 27, pages 355–366. ACM, 1998.
- [16] S.-O. Chan, I. Diakonikolas, G. Valiant, and P. Valiant. Optimal algorithms for testing closeness of discrete distributions. In *SODA*, pages 1193–1203, 2014.
- [17] S. Chaudhuri, G. Das, M. Datar, R. Motwani, and V. Narasayya. Overcoming limitations of sampling for aggregation queries. In *ICDE*, pages 534–542. IEEE, 2001.
- [18] S. Chaudhuri, R. Motwani, and V. Narasayya. Random sampling for histogram construction: How much is enough? In *ACM SIGMOD Record*, volume 27, pages 436–447. ACM, 1998.
- [19] Y. Chen and K. Yi. Two-level sampling for join size estimation. In *Proceedings of the 2017 ACM International Conference on Management of Data*, pages 759–774. ACM, 2017.
- [20] T. H. Cormen. *Introduction to algorithms*. MIT press, 2009.
- [21] C. Daskalakis, I. Diakonikolas, R. O'Donnell, R. A. Servedio, and L.-Y. Tan. Learning sums of independent integer random variables. In *FOCS*, pages 217–226. IEEE, 2013.
- [22] B. Ding, S. Huang, S. Chaudhuri, K. Chakrabarti, and C. Wang. Sample + seek: Approximating aggregates with distribution precision guarantee. In *SIGMOD*, 2016.
- [23] D. Fisher, I. Popov, S. Drucker, and m.c. Schraefel. Trust me, i'm partially right. In *CHI*, page 1673, New York, New York, USA, may 2012. ACM Press.
- [24] V. Ganti, M.-L. Lee, and R. Ramakrishnan. Icicles: Self-tuning samples for approximate query answering. In *VLDB*, volume 176, 2000.
- [25] A. L. Gibbs and F. E. Su. On choosing and bounding probability metrics. *International statistical review*, 70(3):419–435, 2002.
- [26] P. Hanrahan. Analytic database technologies for a new kind of user: The data enthusiast. In *SIGMOD*, pages 577–578, New York, NY, USA, 2012. ACM.
- [27] J. M. Hellerstein, P. J. Haas, and H. J. Wang. Online aggregation. *ACM SIGMOD Record*, 26(2):171–182, jun 1997.
- [28] W.-C. Hou, G. Ozsoyoglu, and B. K. Taneja. Processing aggregate relational queries with hard time constraints. In *ACM SIGMOD Record*, volume 18, pages 68–77. ACM, 1989.
- [29] I. F. Ilyas, G. Beskales, and M. A. Soliman. A survey of top-k query processing techniques in relational database systems. *ACM Comput. Surv.*, 40(4), 2008.
- [30] Y. E. Ioannidis and V. Poosala. Balancing histogram optimality and practicality for query result size estimation. In *ACM SIGMOD Record*, volume 24, pages 233–244. ACM, 1995.
- [31] Y. E. Ioannidis and V. Poosala. Histogram-based approximation of set-valued query-answers. In *VLDB*, volume 99, pages 174–185, 1999.
- [32] H. V. Jagadish, N. Koudas, S. Muthukrishnan, V. Poosala, K. C. Sevcik, and T. Suel. Optimal histograms with quality guarantees. In *VLDB*, volume 98, pages 24–27, 1998.
- [33] U. Jügel, Z. Jerzak, G. Hackenbroich, and V. Markl. M4: a

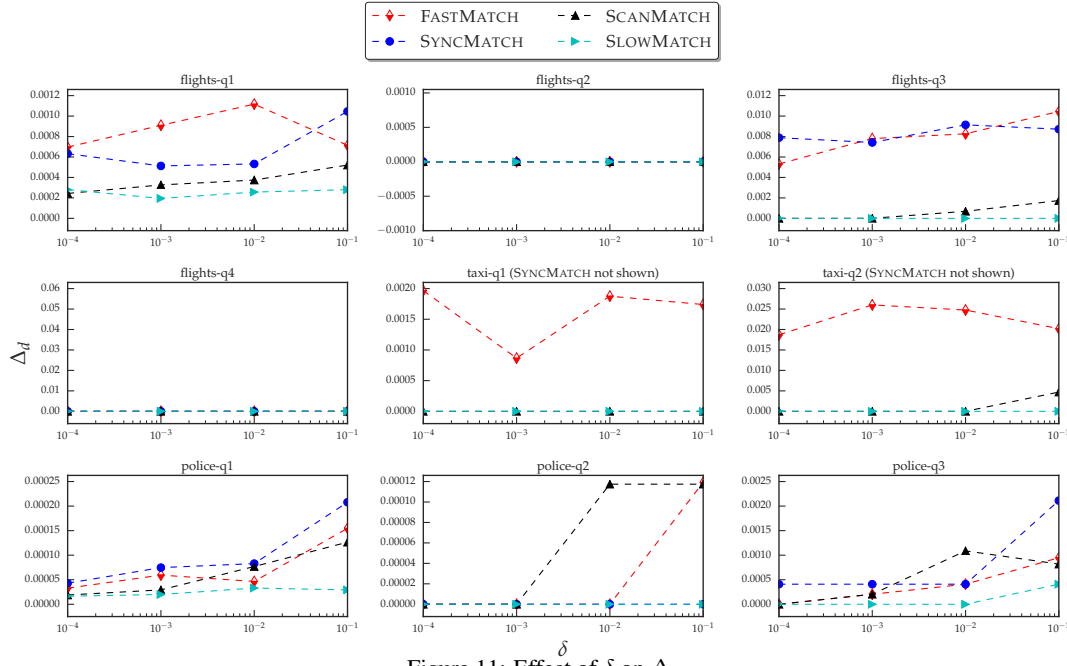


Figure 11: Effect of δ on Δ_d

visualization-oriented time series data aggregation. *PVLDB*, 7(10):797–808, 2014.

- [34] S. Kandel, R. Parikh, A. Paepcke, J. M. Hellerstein, and J. Heer. Profiler: Integrated statistical analysis and visualization for data quality assessment. In *AVI*, pages 547–554. ACM, 2012.
- [35] A. Kim, E. Blais, A. Parameswaran, P. Indyk, S. Madden, and R. Rubinfeld. Rapid sampling for visualizations with ordering guarantees. *PVLDB*, 8(5):521–532, Jan. 2015.
- [36] A. Kim, S. Madden, and A. Parameswaran. Needletail: A system for browsing queries (demo). Technical report, Available at: <http://i.stanford.edu/~adityagp/ntail-demo.pdf>, 2014.
- [37] L. D. Lins, J. T. Klosowski, and C. E. Scheidegger. Nanocubes for real-time exploration of spatiotemporal datasets. *IEEE TVCG*, 19(12):2456–2465, 2013.
- [38] R. J. Lipton, J. F. Naughton, and D. A. Schneider. *Practical selectivity estimation through adaptive sampling*, volume 19. ACM, 1990.
- [39] R. J. Lipton, J. F. Naughton, D. A. Schneider, and S. Seshadri. Efficient sampling strategies for relational database operations. *Theoretical Computer Science*, 116(1):195–226, 1993.
- [40] Z. Liu and J. Heer. The effects of interactive latency on exploratory visual analysis. *IEEE TVCG*, 20(12):2122–2131, 2014.
- [41] Z. Liu, B. Jiang, and J. Heer. immens: Real-time visual querying of big data. In *CGF*, volume 32, pages 421–430. Wiley Online Library, 2013.
- [42] M. Matsumoto and T. Nishimura. Mersenne twister: a 623-dimensionally equidistributed uniform pseudo-random number generator. *ACM Transactions on Modeling and Computer Simulation (TOMACS)*, 8(1):3–30, 1998.
- [43] C. McDiarmid. On the method of bounded differences. *Surveys in combinatorics*, 141(1):148–188, 1989.
- [44] D. Moritz, D. Fisher, B. Ding, and C. Wang. Trust, but verify: Optimistic visualizations of approximate queries for exploring big data. In *CHI*, pages 2904–2915. ACM, 2017.
- [45] B. Mozafari. Approximate query engines: Commercial challenges and research opportunities. In *SIGMOD*, pages 521–524. ACM, 2017.
- [46] B. Nichols, D. Buttlar, and J. Farrell. *Pthreads programming: A POSIX standard for better multiprocessing*. "O'Reilly Media, Inc.", 1996.
- [47] Y. Park, M. Cafarella, and B. Mozafari. Visualization-aware sampling for very large databases. In *ICDE*, pages 755–766. IEEE, 2016.
- [48] P. Pirolli and S. Card. The sensemaking process and leverage points for analyst technology as identified through cognitive task analysis. In *Proceedings of international conference on intelligence analysis*, volume 5, pages 2–4, 2005.
- [49] C. Qin and F. Rusu. Pf-ola: a high-performance framework for parallel online aggregation. *Distributed and Parallel Databases*, 32(3):337–375, 2014.
- [50] S. Rahman, M. Aliakbarpour, H. K. Kong, E. Blais, K. Karahalios, A. Parameswaran, and R. Rubinfeld. I’ve seen “enough”: Incrementally improving visualizations to support rapid decision making. In *VLDB*, 2017.
- [51] C. Ré, N. N. Dalvi, and D. Suciu. Efficient top-k query evaluation on probabilistic data. In *ICDE*, pages 886–895, 2007.
- [52] T. Siddiqui, A. Kim, J. Lee, K. Karahalios, and A. Parameswaran. Effortless data exploration with zenvisage: an expressive and interactive visual analytics system. *PVLDB*, 10(4):457–468, 2016.
- [53] M. A. Soliman, I. F. Ilyas, and K. C. Chang. Top-k query processing in uncertain databases. In *ICDE*, pages 896–905, 2007.
- [54] C. Stolte, D. Tang, and P. Hanrahan. Polaris: A system for query, analysis, and visualization of multidimensional relational databases. *IEEE TVCG*, 8(1):52–65, 2002.
- [55] M. Vartak, S. Rahman, S. Madden, A. Parameswaran, and N. Polyzotis. Seedb: efficient data-driven visualization

- recommendations to support visual analytics. *PVLDB*, 8(13):2182–2193, 2015.
- [56] B. Waggoner. L p testing and learning of discrete distributions. In *ITCS*, pages 347–356. ACM, 2015.
- [57] H. Wickham. *ggplot2: elegant graphics for data analysis*. Springer, 2016.
- [58] K. Wu, E. Otoo, and A. Shoshani. Compressed bitmap indices for efficient query processing. *Lawrence Berkeley National Laboratory*, 2001.
- [59] K. Wu, K. Stockinger, and A. Shoshani. Breaking the curse of cardinality on bitmap indexes. In *Scientific and Statistical Database Management*, pages 348–365. Springer, 2008.
- [60] S. Wu, B. C. Ooi, and K.-L. Tan. Continuous sampling for online aggregation over multiple queries. In *SIGMOD*, pages 651–662. ACM, 2010.
- [61] Y. Wu, B. Harb, J. Yang, and C. Yu. Efficient evaluation of object-centric exploration queries for visualization. *PVLDB*, 8(12):1752–1763, 2015.
- [62] K. Zeng, S. Agarwal, A. Dave, M. Armbrust, and I. Stoica. G-ola: Generalized on-line aggregation for interactive analysis on big data. In *SIGMOD*, pages 913–918. ACM, 2015.

APPENDIX

A. EXTENSIONS

A.1 Generalizing Problem Description

A.1.1 SUM aggregations

While we do not consider it explicitly in this paper, in [22], the authors describe how to perform SUM aggregations with ℓ_2 distributional guarantees via *measure-biased sampling*. Briefly, a measure-biased sample for some attribute Y involves sampling each tuple t in T , where the probability of inclusion in the sample is proportional t 's value of Y . FastMatch can also leverage measure-biased samples in order to match bar graphs generated via the following types of queries:

```
SELECT X, SUM(Y) FROM T
WHERE Z = zi GROUP BY X
```

As in Definition 1, Z is the candidate attribute and X is the grouping attribute for the x-axis. One measure-biased sample must be created per measure attribute Y the analyst is interested in, so if there are n such attributes, we require an additional n complete passes over the data for preprocessing. When matching bar graphs generated according to the above template, FastMatch would simply use the measure-biased sample for Y and pretend as if it were matching visualizations generated according to Definition 1; that is, it would use COUNT instead of SUM. There is nothing special about the ℓ_2 metric used in [22], and the same techniques may be used by FastMatch to process queries satisfying Guarantees 1 and 2.

A.1.2 Candidates based off arbitrary boolean predicates

In order to support candidates based off boolean predicates such as $Z^{(1)} = z_i^{(1)} \wedge Z^{(2)} = z_j^{(2)}$, FastMatch needs a way to estimate the number of active tuples in a block for the purposes of applying AnyActive block selection. In this case, simple bitmap indexes with one bit per block are not enough. We may instead opt to use

the slightly costlier *density maps* from [?]. We refer readers to that paper for a description of how to estimate the number of tuples in a block satisfying an arbitrary boolean predicate. Even if different candidates share some of the same tuples, our guarantees still hold since HistSim uses a union bound to upper bound the probability that a guarantee is violated.

A.1.3 Multiple attributes in GROUP BY clause

In the case where the analyst wishes to use multiple attributes $X^{(1)}, X^{(2)}, \dots, X^{(n)}$ to generate the support of our histograms generated via Definition 1, all of the same methods apply, but we estimate the support $|V_X|$ as

$$|V_{X^{(1)}}| \cdot |V_{X^{(2)}}| \cdot \dots \cdot |V_{X^{(n)}}|$$

This may be an overestimate if two attribute values, say $x_i^{(1)}$ and $x_j^{(2)}$, never occur together. Our guarantees still hold in this case — overestimating the size of the support can only make the bound in Theorem 1 looser than it could be, which does not cause any correctness issues.

A.1.4 Handling continuous X attributes via binning

If the analyst wishes to use a continuous X , she must simply provide a set of non-overlapping bin ranges, or “buckets” in which to collect tuples. Everything else is still the same.

A.2 Different Types of Guarantees

A.2.1 Allowing Distinct ε_1 and ε_2 for Guarantees 1 and 2

If the analyst believes one of Guarantees 1 and 2 is more important than the other, she may indicate this by providing separate ε_1 for Guarantee 1 and ε_2 for Guarantee 2; HistSim generalizes in a very straightforward way in this case. For example, if Guarantee 2 is more important than Guarantee 1, the analyst may provide ε_1 and ε_2 with $\varepsilon_2 < \varepsilon_1$.

A.2.2 Allowing other distance metrics

We can extend HistSim to work for any distance metric for which there exists an analogue to Theorem 1. For example, there exist such bounds for ℓ_2 distance [22, 56].

A.2.3 Allowing a range of k in input

In some cases, the analyst may not care about the exact number of matching candidates. For example, the analyst may be fine with finding anywhere between 5 and 10 of the closest histograms to a target. In this case, she may specify a range $[k_1, k_2]$, and FastMatch may return some number $k \in [k_1, k_2]$ of histograms matching the target, where k is automatically picked to make it as easy as possible to satisfy Guarantees 1 and 2. For example, in the case $[k_1, k_2] = [5, 10]$, there may be a very large separation between the 7th- and 8th-closest candidates, in which case HistSim can automatically choose $k = 7$, as this likely provides a small δ^{upper} as soon as possible.

A.3 Generalizing to Other System Settings

A.3.1 The case of no indexes

If we do not have bitmap or density map indexes, we may simply run our ScanMatch from Section 5. Although not as performant as FastMatch, it can still be vastly superior to Scan in many cases.